Molecular Crystals and Liquid Crystals Science and Technology. Section A. Molecular Crystals and Liquid Crystals

Publication details, including instructions for authors and subscription information:
http://www.tandfonline.com/loi/gmcl19

Liquid Crystal Inversion Walls Caused by Field Fringing

W. J. Cassarly [a b] & S. J. Young [a c]

[a] GE Astro-Space Division, 230 Goddard Blvd., King of Prussia, PA, 19406

[b] University of Pennsylvania, Moore School of Engineering, Philadelphia, PA, 19104

[c] Princeton University, Princeton, NJ, 08544

Version of record first published: 24 Sep 2006.

To cite this article: W. J. Cassarly & S. J. Young (1992): Liquid Crystal Inversion Walls Caused by Field Fringing, Molecular Crystals and Liquid Crystals Science and Technology. Section A. Molecular Crystals and Liquid Crystals, 210:1, 1-9

To link to this article: http://dx.doi.org/10.1080/10587259208030753

Mol. Cryst. Liq. Cryst., 1992, Vol. 210, pp. 1–9
Reprints available directly from the publisher
Photocopying permitted by license only

Printed in the United States of America

Liquid Crystal Inversion Walls Caused by Field Fringing

W. J. CASSARLY† and S. J. YOUNG

(Received June 19, 1991)

A programmable nematic liquid crystal phase plate is formed by sandwiching a layer of liquid crystal material between two glass substrates, each coated with a transparent electrode. Regions of the liquid crystal layer are independently controlled by patterning the electrode into an array of pixels and addressing each pixel with a separate voltage source. The voltage-controlled reorientation (deformation) of the liquid crystal layer far from the pixel edges is well understood; however, very few investigations of the deformation near a pixel edge have been published. We show that near the pixel edges the deformation decreases monotonically, but a transition region located in the center of the pixel results. The transition region, called a liquid crystal inversion wall, is undesirable for most applications but can be forced to form near the edge of the pixel by adding a pretilt to the surface alignment. We present computer simulation results of the voltage-dependent pixel edge deformations and relate the deformations to the phase profile experienced by a wavefront propagating through the programmable phase plate.

Keywords: nematic liquid crystals, inversion walls, programmable phase plates, field fringing

1 BACKGROUND

An untwisted nematic liquid crystal cell with the molecules initially aligned parallel to the transparent substrates is called a planar-aligned cell.[1] A two-dimensional slice of a planar-aligned cell is pictured in Figure 1a with ellipses used to denote the director, which is the local average orientation of the uniaxial liquid crystal molecules. Transparent electrodes are included to allow the application of a controlling voltage. When no control voltage is applied, strong surface anchoring aligns the molecules parallel to the glass substrates. When a nonzero control voltage is applied, the director attempts to align itself parallel to the electric field lines; however, elastic forces and the substrate boundary conditions limit the reorientation. A conceptual picture of the director reorientation for an intermediate control voltage is shown in Figure 1b. The amount of deformation, and therefore the change in the index of refraction, increases with increasing voltage, which enables analog control of the phase of a linearly-polarized wavefront.

† When this research was performed, both authors were with GE Astro-Space Division, 230 Goddard Blvd., King of Prussia, PA 19406. W. J. Cassarly was also affiliated with the University of Pennsylvania, Moore School of Engineering, Philadelphia, PA 19104. S. J. Young was also affiliated with Princeton University, Princeton, NJ 08544.

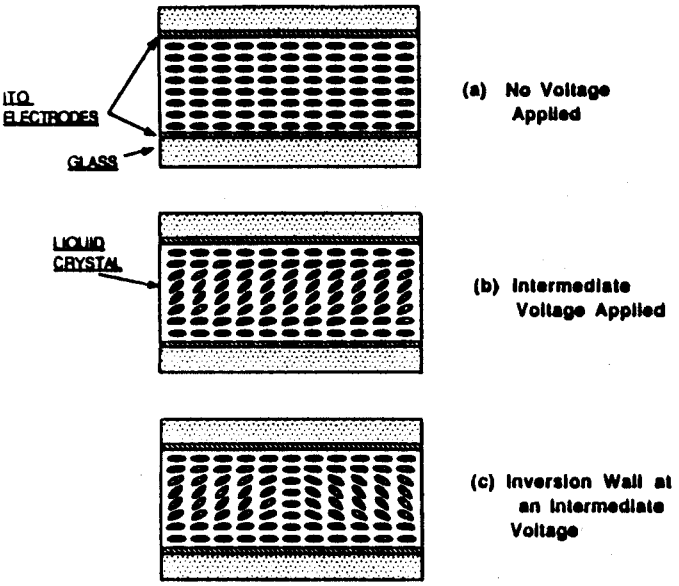

FIGURE 1 Two-dimensional slice of an untwisted, parallel-plate, planar-aligned nematic liquid crystal cell. Voltages are applied with transparent electrodes. (a) shows the cell with no voltage applied, (b) shows the cell with an intermediate voltage applied, and (c) shows the cell with an inversion wall. The director is denoted by the ellipses.

Because the reorientation in nematic liquid crystals is created through induced dipoles, the director profile for a planar-aligned cell can tilt positively or negatively with respect to the substrate surface. Both tilt directions are equally likely if the molecules are all initially aligned parallel to the substrate; however, localized surface perturbations and field fringing effects cause neighboring regions to tilt in opposite directions. When the transition region between oppositely tilted regions is large compared to the size of a liquid crystal molecule,[2] the transition region is called a liquid crystal inversion wall.[3,5,6] A conceptual picture of the inversion wall director profile is shown in Figure 1c.

Previous studies of liquid crystal inversion walls focused upon externally applied homogeneous fields. Brochard,[7] Leger,[8,9] and Rey[10] all investigated liquid crystal inversion walls created by externally applied homogeneous magnetic fields, and Stieb and coworkers[11] and Krishnamurthy[12] studied walls formed by externally applied homogeneous electric fields.

Some investigations of the effect of the inhomogeneous electric field near an electrode edge have been published. Chigrinov and coworkers[13] describe a splay-bend deformation along two of the four electrode edges, and a twist deformation along the other two. More recently, Haas and coworkers[14] have described splay-bend inversion walls which form below a critical voltage (approximately 1.5 to 2 times the Fredericks voltage), as well as a reverse tilt disclination which forms above the critical voltage. Other experimental observations have been made by Cassarly[15] which verify that splay-bend inversion walls form at low voltages, and inversion walls with twist deformations and disclinations form at higher voltages.

A conceptual picture of the splay-bend inversion wall which forms below the

critical voltage in a cell with a finite-width electrode is shown in Figure 2. For most applications uniform deformation is desired so the formation of inversion walls is undesired. To provide a preferred tilt direction and therefore minimize the occurrence of inversion walls, liquid crystal cells are prepared with a small surface pretilt. This forces the inversion wall to form near one of the electrode edges.

In this paper, we present computer simulation results which confirm the creation of liquid crystal inversion walls near an electrode edge and demonstrate the effect of a surface pretilt. Only voltages below the critical voltage are considered. The director profiles for low voltages and the corresponding index of refraction profiles are described. To begin the discussion, we first describe the computer simulation.

2 COMPUTER-AIDED, LOW-VOLTAGE WALL MODEL

The director profile for the deep interior of a pixel is described by Deuling's[16] results. However, these results do not properly describe the profile in the region of an inversion wall or near the pixel's edges. Closed form solutions of the wall profile for electric field deformations are difficult because of the change in the displacement field as the molecules are rotated. This difficulty is not as severe for magnetic field induced deformations because the change in permeability is much less than the absolute permeability for any director angle. This difference makes magnetic field distortions simpler to model numerically.

To model the inhomogeneous electric field and its effect upon the director profile at the edge of an electrode, we developed a new computer simulation.[17,18] The computer routine iteratively computes the director deformation given a set of electric potential boundary conditions. The routine first begins with a user-entered initial director profile and computes the voltage profile throughout the liquid crystal cell assembly. From the calculated voltage profile, the director profile is updated so that the total free energy[19] is reduced. The voltage profile is then recalculated and the procedure repeated until further changes in the director profile introduce no substantial reduction in the total free energy. Currently, twist deformations are not modeled, and therefore the computer model is restricted to splay and bend

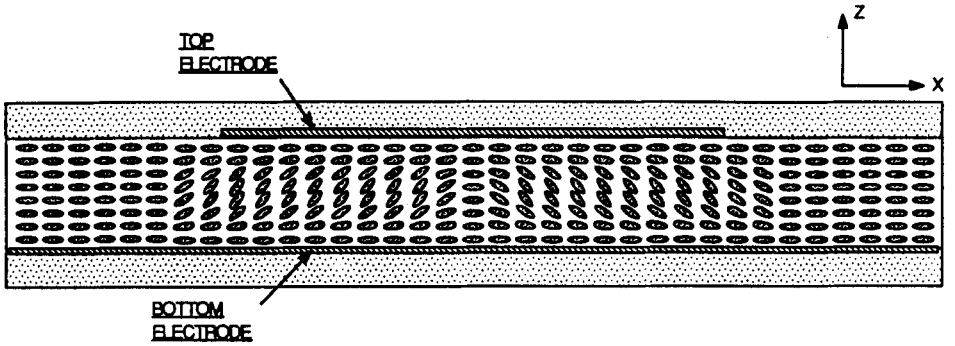

FIGURE 2 Conceptual cross section of a finite-width liquid crystal cell with a wall that separates two regions of equivalent but oppositely tilted directors. The director is denoted by the ellipses. The electrodes are located at $z = 0$ and $z = 6$ μm.

deformation. Other computer-aided modeling of liquid crystal director profiles include Berremans's[20] and van Doorn's[21] investigations of liquid crystal cell dynamics for a homogeneous electric field. More recently, Sammon[22] described a three-dimensional numerical method which incorporates the effects of disclinations as well as cell dynamics.

A cartesian coordinate system with the z axis normal to the cell surfaces is used. The x axis is parallel to the cell surfaces and is in the same direction as the cell buffing. The y axis comes out of the page in all figures here. The director is described by the x and z-dependent tilt and twist angles. The tilt angle, $\theta(x, z)$, is the angle that the projection of the director onto the x-z plane makes with the x axis, and the twist angle, $\omega(x, z)$, is the angle that the projection of the director on to the x-y plane makes with the x axis. In vector form, the director is expressed as $\vec{n} = [\cos\theta(x, z)\cos\omega(x, z), \cos\theta(x, z)\sin\omega(x, z), \sin\theta(x, z)]$. For the no-voltage and no-pretilt case, the molecules are aligned parallel to the x axis. For the low voltages considered, the twist deformations are assumed to be zero so that the director is simply $\vec{n} = [\cos\theta(x, z), 0, \sin\theta(x, z)]$.

Within the iterative computer solution the director tilt is initialized using

$$\theta(x, z) = \theta_m(x)\sin\frac{\pi z}{d}, \tag{1}$$

where d is the liquid crystal cell thickness, $z = 0$ defines the location of the bottom electrode, $z = d = 6$ μm defines the location of the top electrode, $\theta_m(x)$ is the peak tilt as a function of x, and the top electrode extends from $0 < x < x_{\text{edge}}$. To provide known boundary conditions, we assume $\partial\theta/\partial x = 0$ far from the electrode edge, $\theta(x, 0) = 0$, and $\theta(x, d) = 0$. The liquid crystal material constants used are $k_{11} = 1.42 \times 10^{-11}$ N/m^2, $k_{33} = 4.00 \times 10^{-11}$ N/m^2, $\varepsilon_e = 20\ \varepsilon_{fs}$, $\varepsilon_o = 5\ \varepsilon_{fs}$, $\varepsilon_{fs} = 8.854 \times 10^{-12}$ F/m, $n_e = 1.742$, and $n_o = 1.518$. Materials such as BDH E63 and BDH E7 can be modeled with these constants. The surrounding substrate is assumed to be a nonconductive material, such as glass, with a relative dielectric permittivity of 2.3.

3 SIMULATION RESULTS

In Section 3.1 we describe the director profile near the electrode edge. To provide results in a form related to easily-observed experimental quantities, Section 3.2 relates the director profile to the index of refraction profile. In Section 3.3 we describe the director profile for a cell with an inversion wall. Section 3.4 shows that the introduction of a pretilt forces a pseudo-inversion wall to form near the electrode edge, and discusses the index profiles that result from different pretilts.

3.1 Edge Profile with No Pretilt

For the case where the liquid crystal inversion wall forms far from the electrode edge, the amount of deformation decreases monotonically outside the electrode as

shown in Figure 3. The computer simulation results shown are for the case where the top electrode extends from $x = -\infty$ to $x = 30$ μm and the applied voltage is 1.66 Volts. For the case of a finite-width electrode, the director tilts in the positive direction near one electrode edge and in the negative direction near the other edge. For an ideal cell with no pretilt the magnitude of the director profile is identical at both edges. Figure 3 depicts the type of electrode-edge director profile described by Chigrinov[13] but is calculated without the small angle approximations used by Chigrinov.

3.2 Plane Wavefront Illumination

A plane wavefront which passes through a thin liquid crystal cell experiences an index of refraction profile which is uniform throughout most of the cell but varies spatially near the electrode edge or near an inversion wall. For a thin layer of liquid crystal, diffraction within the liquid crystal can be neglected and the effective index of refraction is equal to the average index for a given value of x. For optical processing and beam control applications, the liquid crystal layer can be considered as a polarization-dependent, infinitely-thin, programmable phase transparency. Crossed polarizers can be used to form a programmable amplitude transparency.

The liquid crystal index of refraction, $n(x, z)$, is related to the director tilt through the relationship

$$n(x, z) = \frac{n_e}{\sqrt{1 + \left[\frac{n_e^2}{n_o^2} - 1\right] \sin^2\theta(x, z)}}. \tag{2}$$

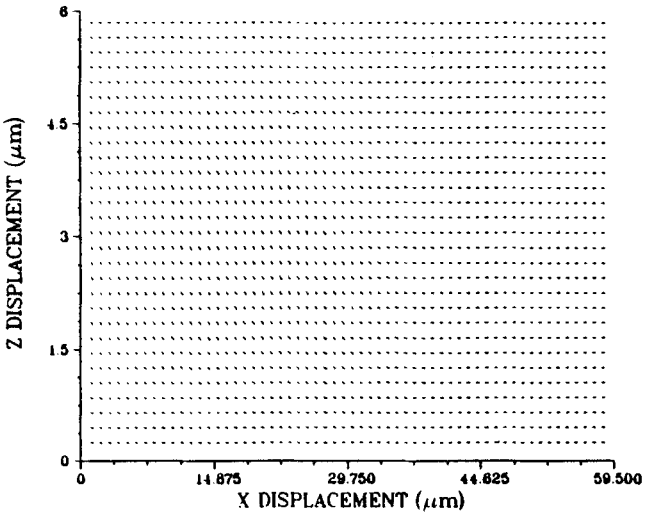

FIGURE 3 Calculated electrode edge director profile when the tilt in the center of the pixel is nearly parallel to the field fringing direction. The voltage is 1.66 volts and the local tilt direction is denoted by the angle of the small lines. The electrode extends from $x = -\infty$ to $x = 30$ μm and is located at $z = 6$ μm.

With $\theta(x, z) = 0$ throughout the cell, the index of refraction for all x is equal to n_e. For a given x, the absolute value of the change in the index of refraction, $\Delta n_{avg}(x)$, is

$$|\Delta n_{avg}(x)| = \left| n_e - \int_0^d n(\theta(x, z))dz \right|. \quad (3)$$

The $|\Delta n_{avg}(x)|$ profiles near an electrode edge for four example voltages are shown in Figure 4. The change increases with voltage and decreases monotonically outside the electrode. It is approximately zero for voltages below threshold,[23] except near the electrode edge, where transverse electric fields serve to rotate the liquid crystal molecules somewhat, even below the threshold voltage.

3.3 Liquid Crystal Inversion Walls

To confirm that a liquid crystal inversion wall is a stable director deformation in a planar cell with homogeneous alignment, an infinitely wide electrode with a quasi-inversion wall was used for the starting conditions. The initial conditions in this simulation were as follows: $|\theta_m(x)|$ equaled a constant for $|x - 30\ \mu m| > 5\ \mu m$; $\theta_m(x)$ was negative for $-\infty < x < 25\ \mu m$; $\theta_m(x)$ was positive for $35\ \mu m < x < \infty$; and $\theta_m(x)$ varied linearly in the 10 μm wide transition region. The computer simulation converged to stable director deformations.

The $|\Delta n_{avg}(x)|$ profiles for four example voltage simulations are shown in Figure 5. The profiles show that a liquid crystal inversion wall is indeed a stable director

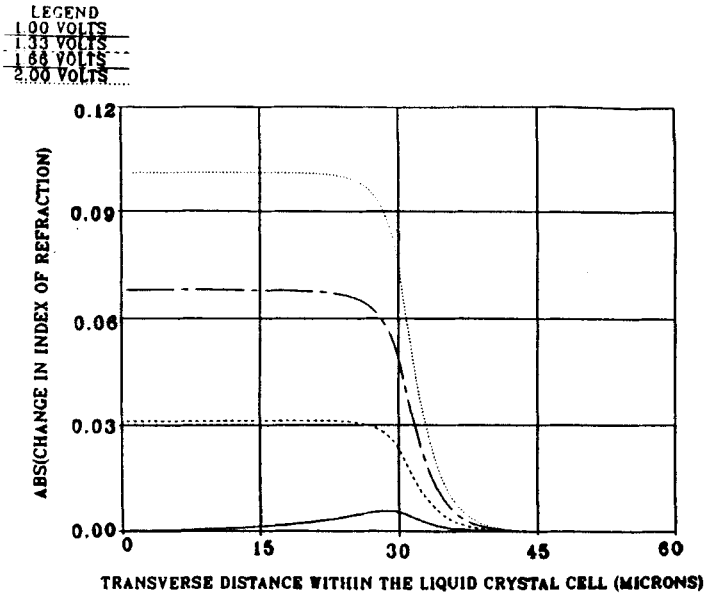

FIGURE 4 Calculated average index of refraction profile for a pixel edge with no inversion wall. Voltages equal to 1.0, 1.33, 1.66, and 2.0 are shown.

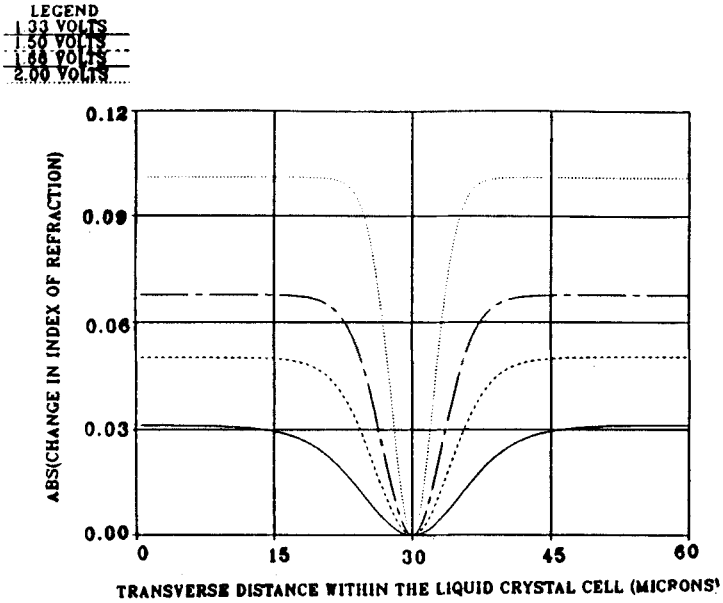

FIGURE 5 Calculated average index of refraction profile for several liquid crystal inversion walls. Voltages equal to 1.33, 1.50, 1.66, and 2.0 are shown.

deformation. The profiles also show that $|\Delta n_{avg}(x)|$ increases monotonically with voltage for any given value of x, and the wall width decreases with increasing voltage.

3.4 The Effect of Pretilt

With a pretilt, a liquid crystal inversion wall is not a stable director deformation for the case of an infinitely-wide, constant-potential electrode. This was verified with the computer simulation. We also observed that for a given cell thickness and voltage, $|\Delta n_{avg}(x)|$ is larger for a pretilted cell than for a cell without pretilt.

By adding a small surface pretilt opposite to the tilt direction for the finite electrode case shown in Figure 3, the inversion wall forms near the electrode edge. Computer simulation index profile results for the case of an applied voltage of 1.66 Volts and surface layer pretilts of 1.5°, 3.0°, and 6.0° are shown in Figure 6. The inversion wall index profile under the electrode for the 1.5° pretilt case is similar to an inversion wall centered around $x \approx 27$ μm. The left half of the inversion wall's $|\Delta n_{avg}(x)|$ profile is similar to the profile described in Figure 5, but the right half is different because of the electric field fringing.

With no pretilt, the inversion wall forms midway between the electrode edges in an ideal cell. When the pretilt is large enough, such as the 6° pretilt case, the edge-induced director profile distortion becomes a reduction in the director angle reorientation rather than an inversion wall. This reduction in director reorientation creates a 'dip' in the index profile. This occurs because the transverse voltage at this electrode is no longer able to overcome the pretilt and force the director angle below zero. Thus a true inversion wall, which occurs when the director angle does

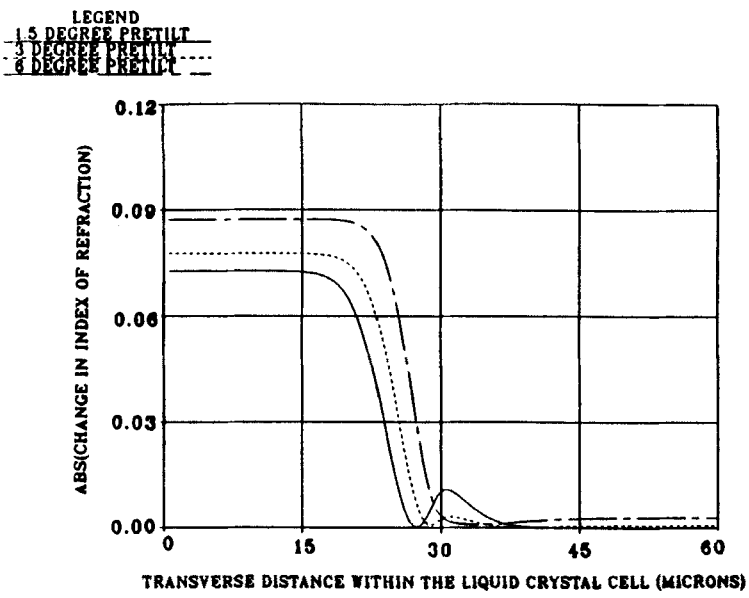

FIGURE 6 Calculated average index of refraction profile for a liquid crystal cell with an inversion wall and a surface pretilt. The voltage equals 1.66 volts; and pretilts of 1.5°, 3°, and 6° are shown.

not go below zero at some point, does not form as it did for the 1.5° and 3° pretilt cases.

We call the dip, plus the region of rapid director tilt change around it, a pseudo-inversion wall. Figure 6 shows that the index of refraction falloff forms monotonically closer to the electrode edge as the pretilt increases. The dip profile is voltage dependent because larger voltages introduce larger transverse electric fields.

4 DISCUSSION

The simulation results demonstrate that the $|\Delta n_{avg}(x)|$ profile exhibits a monotonic falloff in the region near one electrode edge. At this electrode edge but under the electrode, the deformation is slightly less than the deformation in the center of the cell. In addition, the deformation outside the electrode is not zero. The last two effects makes the size of the uniformly distorted region different than the actual electrode size.

Small pretilts can be added to force the inversion wall to form near one of the electrode edges. As the pretilt increases, however, the wall forms closer and closer to the electrode edge. With a large enough pretilt, the edge-induced director profile distortion becomes a reduction in the director angle reorientation rather than a transition between regions of opposite tilt, an effect we call a pseudo-inversion wall. At the electrode edge where the inversion wall or pseudo-inversion wall forms, the uniformly deformed region is distorted further in from the end of the electrode than at the opposite edge.

The effect of electrode edge field fringing has been discussed using the results

of a computer simulation. Inversion walls and pseudo-inversion walls are shown to be stable director deformations in untwisted, planar-aligned liquid crystal cells. These results should prove useful in describing the resolution limit of liquid crystal spatial modulation devices.

References

1. Planar alignment is sometimes called homogeneous alignment.
2. The size of a liquid crystal molecule is on the order of a few to tens of angstroms.
3. Demus and Richter[4] summarize the different wall types that are possible for nematic liquid crystal cells. The computer-aided modeling that we present focuses upon splay-bend walls.
4. D. Demus and L. Richter, *Texture of Liquid Crystals*, (Verlag Chemie, Weinheim, NY, 1978).
5. W. Helfrich, *Phys. Rev. Lett.*, **21**, (22) 1518 (1968).
6. P. G. deGennes, *The Physics of Liquid Crystals*, (Clarendon Press, Oxford, 1974).
7. F. Brochard, *Le Jou. De Phys.*, **33**, (5–6) 607 (1972).
8. L. Leger, *Sol. State Comm.*, **11**, 1499 (1972).
9. L. Leger, *Mol. Cryst. Liq. Cryst.*, **24**, 33 (1973).
10. A. D. Rey, *Liq. Cryst.*, **7**, (3) 315 (1990).
11. A. Stieb, G. Baur and G. Meier, *Jou. de Phys. Coll.*, **C1–36**,(3) C1–185 (1975).
12. K. S. Krishnamurthy and M. S. Bhate, *Mol. Cryst. Liq. Cryst.*, **128**, 29 (1985).
13. V. G. Chigrinov, I. N. Kompanets and A. A. Vasilev, *Mol. Cryst. Liq. Cryst.*, **55**, 193 (1979).
14. G. Haas, H. Wohler, M. W. Fritsch and D. A. Mlynsji, *SID*, **P18**, 252 (1990).
15. W. J. Cassarly, Ph.D. Dissertation, Univ. of Penn., Phila. (1990).
16. H. J. Deuling, *Mol. Cryst. Liq. Crystal.*, **19**, 123 (1972).
17. S. J. Young, Senior Independent Project, EE Department, Princeton Univ., Princeton, NJ, Jan. (1990).
18. S. J. Young, Senior Independent Project, EE Department, Princeton Univ., Princeton, NJ, May (1990).
19. The free energy is the sum of the elastic energies and the electrostatic energies.
20. D. W. Berreman, *Jou. Appl. Phys.*, **46**, (9) 3746 (1975).
21. C. Z. van Doorn, *Jou. Appl. Phys.*, **46**, (9) 3738 (1975).
22. M. J. Sammon, *Mol. Cryst. Liq. Cryst.*, **89**, 305 (1982).
23. The liquid crystal threshold voltage, the Fredericks voltage, is equal to $\pi\sqrt{k_{11}/\varepsilon_e - \varepsilon_o}$.